

Physical simulation and theoretical analysis of migrating rate of inclusions in aluminum melt in electromagnetic field^①

LI Tian-xiao(李天晓), SHU Da(疏达), XU Zhen-ming(许振明),

SUN Bao-de(孙宝德), ZHOU Yao-he(周尧和)

(School of Materials Science and Engineering, Shanghai Jiaotong University, Shanghai 200030, P. R. China)

[Abstract] Simulation law and physical simulation were used to study the kinematic behavior of inclusions in electromagnetic separation. It was found that velocity of spherical non-metallic particles shares different functions in different Reynolds number range. The function of spherical particle's velocity has been got by confirming the relationship between Reynolds number and resistance coefficient when Reynolds number is 0.2~10. For non-spherical particles, the moving behavior is influenced by shape and orientation while spherical coefficient has nothing to do with the velocity of irregular particles. The influence of orientation of cuboid particle on the electromagnetic expulsive force has been indicated by numerical computation.

[Key words] electromagnetic separation; non-metallic particles; physical simulation; migrating rate

[CLC number] TF111.18; TF114.12

[Document code] A

1 INTRODUCTION

Very small non-metallic inclusions can be removed from aluminum melt by electromagnetic separation^[1~5]. Therefore, it is thought to be a promising way to meet the demand for cleaner melt. Clarifying kinematic law of inclusion movement is necessary to design electromagnetic separating equipment and to develop separating techniques. The shapes of most inclusions in aluminum melt are irregular. The electromagnetic expulsive forces of irregular inclusions were mentioned in Refs.[2,6], but no concrete study about moving behavior of irregular particles has been reported. For spherical particles, the equation of migrating rate used in Ref.[3] was derived from the balance between the electromagnetic expulsive force given by Leenov and Kolin^[7] and Stokes drag force^[8], that is

$$u_{\infty} = \frac{d^2}{24\mu} |\mathbf{J} \times \mathbf{B}| \quad (1)$$

where u_{∞} is the terminal migrating velocity of inclusions, d is the diameter of inclusions, \mathbf{J} is the current density, \mathbf{B} is the magnetic flux density vector, and μ is the viscosity of the fluid.

Reynolds number of inclusions larger than 20 μm can easily reach and exceed 0.2 in electromagnetic separation of aluminum melt. Reynolds number of inclusions less than 20 μm can exceed 0.2 under electromagnetic field of large intensity too. When Reynolds number is larger than 0.2, the Stokes law is not

valid^[8] and Eqn. (1) is not valid, either. However, Eqn. (1) was still used in the studies of electromagnetic separation^[2,9,10]. Therefore, clarifying the migrating rate of inclusions when Reynolds number is larger than 0.2 is essential. This paper is concerned with studying electromagnetic expulsive force and kinematic law of non-metallic inclusion moving in aluminum melt by physical simulation and numerical calculation, which offers theoretical basis for electromagnetic separation of aluminum melt.

2 THEORETICAL BACKGROUND

It is difficult to study the kinematic law of inclusion movement in aluminum melt directly. Therefore, physical simulation is used to study the movement of non-metallic particles. In electromagnetic field, non-metallic particle movements in aluminum melt and in electrolyte share the same equation:

$$\rho_f \frac{\partial u}{\partial t} = (\rho_p - \rho_f)g + \frac{3}{4}B \times J - 18 \frac{\mu}{d^2} \quad (2)$$

where ρ_f and ρ_p are the densities of liquid and particles, respectively, u is the velocity of particles, μ is the viscosity of liquid, d is the diameter of non-metallic particles, and g is the acceleration of gravity.

According to Eqn. (2) and similarity principle^[11], two decisive characteristic parameters can be obtained:

① **[Foundation item]** Project (59871029) supported by the National Natural Science Foundation of China and project (G1999064900) supported by the National Key Fundamental Research Project ("973")

[Received date] 2000- 02- 28; **[Accepted date]** 2000- 06- 05

$$Re = \frac{ud_p\rho}{\mu} = \text{const} \quad (3)$$

$$\frac{\Delta Q g d_p}{u^2} = \text{const} \quad (4)$$

Particle movement in electrolyte can be used to simulate inclusion movement in aluminum melt when these two characteristic parameters are the same in the two systems and geometry simulation is kept at the same time.

3 EXPERIMENTAL

Chlorhydric acid solution was used to simulate aluminum melt, transparent plexiglass pipe to simulate separator and polystyrene particles to simulate non-metallic inclusions. The diameter of polystyrene spherical particles was in the range of 0.3~0.7 mm, its density was 1023 kg/m³. The density of chlorhydric acid solution was adjusted to make the particles suspend in it. The transparent plexiglass pipe (200 mm × 20 mm × 8 mm) was placed horizontally to make the direction of DC perpendicular to the direction of the magnetic field. The schematic diagram of experimental apparatus is shown in Fig. 1.

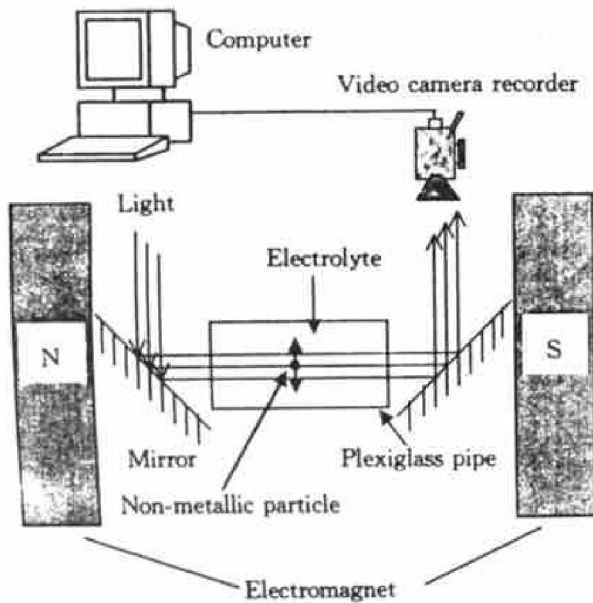


Fig. 1 Schematic diagram of velocity measuring

The electrodes were placed at the two ends of the pipe. The DC were in the range of 0~1000 mA. Magnetic field were generated by electromagnet with a cross section of 130 mm × 130 mm and a gas gap of 40~140 mm. Magnetic flux density, B , could be up to 1 T. The two mirrors were perpendicular to each other to keep the output light parallel to the input light. The movement of particles was recorded by Video Camera Recorder at a rate of 25 frames per second. Magnification ratio was measured by a ruler adhered on the pipe. The continuous photos were captured, encoded and cut into one-one photos in a computer so that the position of a particle in any moment

can be known. By testing the relative position of a particle in a certain interval, velocity of particle can be calculated.

In order to study the moving behavior of irregular particles, the polystyrene particles of good sphericity were deformed. Because the density of the particles keep the same under slow deformation, the equivalent diameter of deformed particles can be considered to be the diameter of the original ones. The spherical coefficient of deformed particles can be got by dividing the settling velocity of deformed particles (settling in water at room temperature) by the velocity of the original ones. The influence of spherical coefficient on the velocity of electromagnetic separation can be got by comparing the velocities of the particles before and after deformation, which are measured in experimental apparatus shown in Fig. 1. The diameter of original particles is 0.66 mm. The density of electromagnetic force (EMF) is 534.3 N/m³ in the experiment on deformed particles. One particle of silicate whose density is similar to dilute chlorhydric acid is cut into cuboid of 1.82 mm × 1 mm × 0.6 mm to simulate cuboid inclusions in aluminum melt. The experiment on the cuboid silicate is done by the same experimental method mentioned above to observe its moving behavior in electromagnetic field. The density of EMF in the experiment is 2446.3 N/m³. The initial position of the particle is near the edge of the plexiglass pipe and its length (1.82 mm) direction parallels to the magnetic field, its width direction (1 mm) to DC.

4 RESULTS AND DISCUSSION

4.1 Confirming terminal velocity of spherical particles

Reynolds number is in the range of 4.31~10.57 in Fig. 2(a) and 4.95~9.35 in Fig. 2(b), respectively. It can be seen that the experimental results are not in conformity with the calculated results obtained from Eqn. (1).

If the influence of gravity and buoyancy can be overlooked, drag force and electromagnetic expulsive force exerted on non-metallic particles will keep the balance:

$$C_D \times A_p \times \frac{1}{2} \rho_t u_i^2 = V_p \times \frac{3}{4} B \times J \quad (5)$$

$$A_p = \frac{1}{4} \pi d_p^2, \quad V_p = \frac{1}{6} \pi d_p^3$$

Then Eqn. (5) is transformed to be

$$C_D \rho_t u_i^2 = d_p B \times J \quad (6)$$

where C_D is drag force coefficient of particles, A_p is the area where drag force exerts on, V_p is the volume of a particle. When the function of drag force coefficient is known, the relationship between technical parameters and terminal velocity of particle can be confirmed.

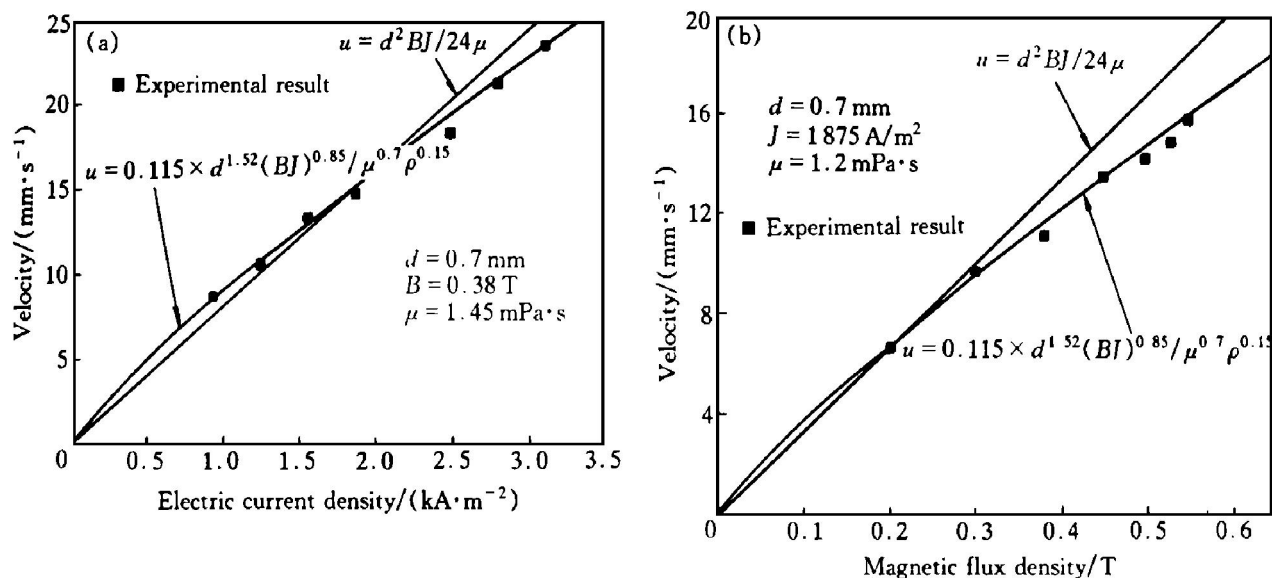


Fig. 2 Relationship between EMF and migrating rate of particle
(a) —Velocity vs electric current density; (b) —Velocity vs magnetic flux density

For different Reynolds number range, the relationship between drag force coefficient and Reynolds number is different:

$$C_D = \frac{24}{Re} \quad Re \leq 0.2^{[8]} \quad (7)$$

$$C_D = \frac{10}{\sqrt{Re}} \quad 25 \leq Re \leq 500^{[12]} \quad (8)$$

There is no proper equation to indicate the relationship between Reynolds number and drag force coefficient when Reynolds number is in the range of 0.2 ~ 25. According to the exponential relationship between drag force coefficient and Reynolds number shown in Eqns. (7) and (8), the relationship between them are supposed to be exponential as Reynolds number in the range of 1~ 10. Based on the exponential relationship between them and the change tendency of experimental result shown in Fig. 2, that is the terminal velocity of particles is linear with $(BJ)^{0.85}$, their relationship can be expressed as follows:

$$C_D = \frac{12.7}{Re^{0.82}} \quad 1 \leq Re \leq 10 \quad (9)$$

Therefore, the terminal velocity of particles can be calculated by

$$u = 0.115 \frac{d^{1.52}}{\mu^{0.7} \rho^{0.15}} (BJ)^{0.85} \quad (10)$$

As seen in Fig. 2, the calculated results by Eqn. (10) and experimental results are almost identical. The same results were obtained in other experiments in which Reynolds number fell in the same range.

In order to check whether Eqn. (10) can be used when Reynolds number is less than 1, another experiment in which Reynolds number is in the range of 0.21~ 0.84 has been done. The result is shown in Fig. 3. It can be seen that the curve calculated by Eqn. (10) is identical to the experimental result

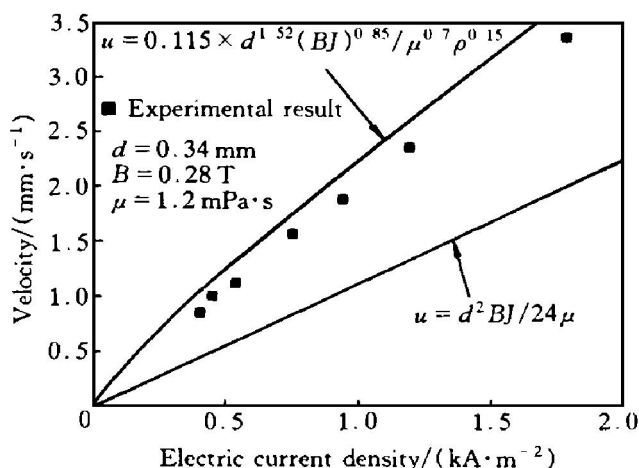


Fig. 3 Relationship between EMF and migrating rate of particle

approximately, while the curve by Eqn. (1) deviates from the result obviously. Thus, Eqn. (10) can be used to calculate the migrating rate of inclusions when Reynolds number is in the range of 0.2~ 1.

In aluminum melt (viscosity of melt is chosen to be 2.5×10^{-3} Pa·s), for spherical inclusion with diameter of 50 μ m, if its Reynolds number is larger than 10, the EMF density must be larger than 5×10^6 N/m³ which is difficult to reach in industrial manufacture. For inclusion of 10 μ m, if its Reynolds number is larger than 10, the EMF density must be larger than 6.25×10^8 N/m³, which is difficult to reach even in laboratory. Therefore, the situation of Reynolds number larger than 10 is not mentioned.

4.2 Moving behavior of irregular particles

Shape coefficient in electromagnetic field is defined by dividing the velocity of deformed particles moving in electromagnetic field by the velocity of spherical particle with the same volume under the

same condition. The relationship between the velocity of deformed particle and the spherical coefficient of the particle is shown in Table 1. It is seen that the velocity of deformed particles can be larger or less than that of the spherical particle with the same volume in electromagnetic field while all deformed particles move slower than the spherical ones when settling in water. That's to say the shape coefficient in electromagnetic field has nothing to do with the spherical coefficient in gravity settlement. The velocity of deformed particle can be influenced by the shape and direction of the particle.

Table 1 Influence of particle shape on velocity

Spherical coefficient	Velocity / (mm·s ⁻¹)	Shape coefficient in electromagnetic field
1	6.57	1
0.43	7.45	1.13
0.54	6.86	1.04
0.56	6.50	0.99
0.63	7.07	1.07
0.68	4.78	0.73
0.79	5.75	0.88
0.91	8.73	1.33

Fig. 4 shows the schematic of a balanced cuboid particle moving in the electrolyte, the two sides are the edges of plexiglass pipe. When the particle leaves one side of the pipe, the cuboid particle rotated until it reaches balance in the middle of the pipe. When it reaches near the other side, it rotates again in the direction opposite to the original orientation as it stopped at the edge of the pipe. When the direction of EMF is changed, the particle moves in the opposite direction but the rotating law and balance orientation are the same. While keeping balance, the angle between the direction of the particle width and DC is

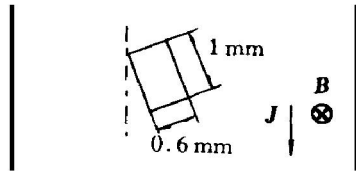


Fig. 4 Balance orientation of cuboid particle

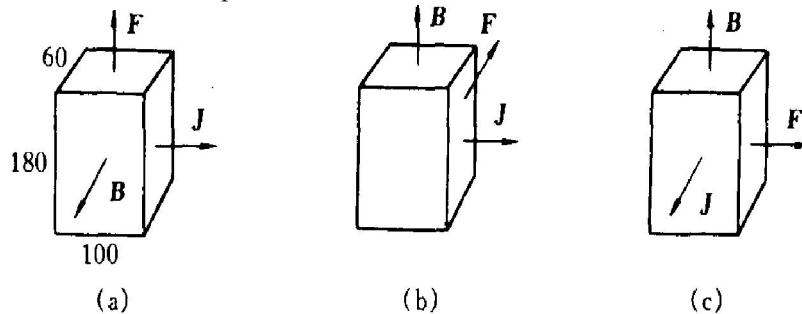


Fig. 5 Schematic of orientation of calculated particle

29°. The phenomenon indicates that moving behavior of irregular particle in electromagnetic field is relevant to the orientation of the particle.

Because of the difference in electricity between the non-metallic inclusions and the aluminum melt, electric streamlines near the inclusion are deformed. Non-uniform electromagnetic field near the inclusion brings the turbulence of the melt. The electromagnetic expulsive force exerted on the inclusion can be calculated by the following numerical model.

The control function of electric field is Laplace Function:

$$\nabla^2 \phi = 0 \quad (11)$$

The distribution of electric density in the melt can be calculated by

$$J_f = -\sigma_f \nabla \phi \quad (12)$$

The turbulence of the melt can be described by N-S function and continuity function:

$$\rho_f \mathbf{v} \cdot \nabla \mathbf{v} = -\nabla p + \mathbf{f} + \mu_f \nabla^2 \mathbf{v} \quad (13)$$

$$\nabla \cdot \mathbf{v} = 0 \quad (14)$$

The electric field and fluid field are calculated continually by the method of finite element. After the pressure distribution in the melt is known, the electromagnetic expulsive force can be got by integral of the pressure distribution along the surface of the inclusion:

$$\mathbf{F} = \iint p \, d\mathbf{s} \quad (15)$$

The parameters used in the calculation are: $J_0 = 1 \times 10^6 \text{ A/m}^2$, $B_0 = 1 \text{ T}$, $\sigma_f = 2.95 \times 10^6 \text{ S/m}$, $\rho_f = 2.37 \times 10^3 \text{ kg/m}^3$, $\mu_f = 2.5 \times 10^{-3} \text{ Pa}\cdot\text{s}$. The size of the calculated cuboid is $180 \mu\text{m} \times 100 \mu\text{m} \times 60 \mu\text{m}$. Thus $J_0 B_0 V$ which represents the electromagnetic force exerted on the displaced volume of fluid is $1.08 \times 10^{-6} \text{ N}$. The electromagnetic expulsive forces exerted on the cuboid particle in three orientations as shown in Fig. 5 were calculated.

For the orientations shown in Fig. 5, the calculated results are 0.95412×10^{-6} , 0.70505×10^{-6} and $0.76487 \times 10^{-6} \text{ N}$, respectively, so that $F/J_0 B_0 V$ are 0.8834, 0.6258 and 0.7082, respectively. It is found that the expulsive forces exerted on the cuboid particle are not the same in different orientations. As shown in Fig. 4, the expulsive force exerted on the particle in original orientation is $1.579 \times$

10^{-3} N, and it is 1.732×10^{-3} N if the particle turns 90° anticlockwise. Therefore, the particle has a rotating tendency when it moves in electromagnetic field. As the particle turned, the expulsive force became large while the drag force became large too. At one angle, the two forces reached balance as shown in Fig. 4.

5 CONCLUSIONS

1) Drag force coefficient and velocity of particles in electromagnetic field when Reynolds number is in the range of 0.2~10 can be calculated by the following equation:

$$u = 0.115 \frac{d^{1.52}}{\mu^{0.7} \rho^{0.15}} (BJ)^{0.85}$$

$$0.2 \leq Re \leq 10$$

2) The velocity of irregular particles in electromagnetic field can not be modified by spherical coefficient.

3) The moving behavior of irregular particles is influenced by shape and orientation. Numerical calculation and physical simulation indicate that cuboid particle rotates to one balance state while moving in electromagnetic field.

[REFERENCES]

- [1] El-Kaddah N, Patel A D and Natarajan T T. The electromagnetic filtration of molten aluminum using an induced-current separator [J]. JOM, 1995, 5: 46.
- [2] Patel A D and El-Kaddah N. Kinetics of inclusion removal from molten aluminum under an applied alternating magnetic field [J]. Huglen R. Light Metals 1997, TMS, Warrendale, PA, 1997, 1013.
- [3] Park J-P, Morihira A, Sassa K, et al. Elimination of nonmetallic inclusions using electromagnetic force [J]. Testur to Hagane, 1994, 80: 31.
- [4] SHU D, SUN B D, WANG J, et al. Study of electromagnetic separation of nonmetallic inclusions from aluminum melt [J]. Metallurgical and Materials Transactions A, 1997, 30A(11): 2979.
- [5] ZHONG Yurbo, REN Zhong-ming, DENG Kang, et al. Separation of inclusions from liquid metal contained in a triangle/square pipe by travelling magnetic field [J]. Trans Nonferrous Met Soc China, 2000, 10(2): 240.
- [6] Marty P and Alemany A. Theoretical and experimental aspects of electromagnetic separation. Metallurgical applications of magnetohydrodynamics [A]. Proceedings of a Symposium of the IUTAM [C]. The Metals Society, 1982. 245.
- [7] Leenov D and Kolin A. Theory of Electromagnetophoresis. I. magnetohydrodynamic forces experienced by spherical and symmetrically oriented cylindrical particles [J]. Journal of Chemical Physics, 1954, 22: 683.
- [8] Douglas J F, Gasiorek J M and Swaffield J A. Fluid Mechanics, (in Chinese), [M]. Beijing: Higher Education Press, 1992. 235.
- [9] Taniguchi S and Brimacombe J K. Theoretical study on the separation of inclusion particles by pinch force from liquid steel flowing in the circular pipe [J]. ISIJ International, 1994, 34: 722.
- [10] ZHONG Yurbo, REN Zhong-ming, DENG Kang, et al. Electromagnetic force parameters during purifying liquid metal by travelling magnetic field [J]. The Chinese Journal of Nonferrous Metals, 1999, 9: 482.
- [11] LIU Yue-yuan, FENG Tie-cheng and LIU Ying-zhong. Basis of Water Dynamics, (in Chinese), [M]. Shanghai: Shanghai Jiaotong University Press, 1990. 2490.
- [12] TONG Qing-li. Theoretical Basis of Two-Phase Flow, (in Chinese), [M]. Beijing: Metallurgical Industry Press, 1982. 43.

(Edited by PENG Chao-qun)